International Conference on Mathematics and Computational Methods Applied to Nuclear Science and Engineering (M&C 2011)
Rio de Janeiro, RJ, Brazil, May 8-12, 2011, on CD-ROM, Latin American Section (LAS) / American Nuclear Society (ANS)
ISBN 978-85-63688-00-2

EXPONENTIALLY-CONVERGENT MONTE CARLO VIA FINITE-ELEMENT TRIAL SPACES

Jim E. Morel, Jared P. Tooley, Brandon J. Blamer
Department of Nuclear Engineering
Texas A&M University
College Station, Texas, USA
morel@tamu.edu; jared_t@tamu.edu; brandonblamer@tamu.edu

ABSTRACT

Exponentially-Convergent Monte Carlo (ECMC) methods, also known as adaptive Monte Carlo and residual Monte Carlo methods, were the subject of intense research over a decade ago, but they never became practical for solving the realistic problems. We believe that the failure of previous efforts may be related to the choice of trial spaces that were global and thus highly oscillatory. As an alternative, we consider finite-element trial spaces, which have the ability to treat fully realistic problems. As a first step towards more general methods, we apply piecewise-linear trial spaces to the spatially-continuous two-stream transport equation. Using this approach, we achieve exponential convergence and computationally demonstrate several fundamental properties of finite-element based ECMC methods. Finally, our results indicate that the finite-element approach clearly deserves further investigation.

Key Words: Adaptive Monte Carlo, Residual Monte Carlo, Finite-Element

1. INTRODUCTION

It is well-known that standard Monte Carlo algorithms reduce statistical errors in proportion to $1/\sqrt{N}$, where N is the number of particle histories that are performed. Using an approach known as adaptive, geometrically-convergent, or residual Monte Carlo, it is possible to reduce statistical errors in proportion to $\exp(-\alpha N)$, where α is a positive constant [1]. When such error reduction is achieved, solutions can be efficiently obtained with as many digits of accuracy as is desired throughout the problem domain, enabling statistical error to be reduced to the same level as iterative error in deterministic solutions. The efficient reduction of Monte Carlo noise to negligible levels is critical for coupled neutronics-thermal hydraulics simulations where statistical noise in the neutronics solution can contaminate the thermal hydraulics solution. Exponentially-convergent Monte Carlo (ECMC) methods have previously been shown to be practical for finite-dimensional systems such as the discretized radiative diffusion equations [2]. They have also been demonstrated for the continuous neutron transport equation [3, 4], but only for homogeneous 1-D problems using Case eigenfunction-based algorithms impractical for realistic problems. A successful approach was demonstrated for the 3-D spatially-continuous S_n equations using global polynomial trial spaces [5], but further generalizations of the approach were not successful. We believe that the failure of this approach was related to the use of highly oscillatory trial spaces that generated excessive numerical error in the solution. It is the purpose of this paper to introduce an ECMC approach based upon spatial finite-element trial spaces.

This approach has significant advantages relative to previous approaches. First, one can achieve convergence of the solution without increasing the oscillatory nature of the trial space by refining the mesh (h-refinement). Global polynomial trial spaces become increasingly oscillatory as the order is increased. Second, finite-element trial spaces can be used to efficiently represent fully-realistic solutions. Third, the use of finite-element spaces will enable the seamless coupling of Monte Carlo transport physics with other physics components in multiphysics calculations.

As a first step toward more general algorithms, we use piecewise-linear discontinuous trial spaces and apply them to the spatially-continuous two-stream transport equations. These equations are very similar to the slab-geometry S_2 equations, and they similarly require only a spatial discretization to be solved. Using this approach, we achieve exponential convergence and computationally demonstrate several fundamental properties of finite-element based ECMC methods. Finally, we conclude that the finite-element approach clearly deserves further investigation.

The remainder of this paper is organized as follows. First we describe the basic theme of ECMC methods. Next we discuss the two-stream equations and describe our particular finite-element implementation of an ECMC method for those equations. Computational results are next presented, followed by conclusions and recommendations for further work.

2. Residual Monte Carlo

The central theme of residual Monte Carlo is straightforward. Assume that one can use a standard Monte Carlo algorithm to solve the continuous transport equation, which we express in the following form:

$$\mathbf{L}\psi = q \quad , \tag{1}$$

where $\mathbf{L}$ denotes the transport operator with appropriate boundary conditions, ψ denotes the angular flux solution, and q denotes the inhomogeneous source. In a standard Monte Carlo algorithm, one performs a set of batches with each batch estimating the solution to Eq. (1). The final solution is just the average of the independent batch solutions. In a residual Monte Carlo algorithm, the first batch is identical to that for standard Monte Carlo. Let us denote that solution estimate by $\psi^{(1)}$. The next batch does not yield another estimate of the solution, but rather yields an estimate of the additive error in $\psi^{(1)}$. Let $\epsilon^{(1)}$ denote this error, then

$$\epsilon^{(1)} \equiv \psi_e - \psi^{(1)} \quad , \tag{2}$$

where ψ_e denotes the exact angular flux solution. It is easily shown that $\epsilon^{(1)}$ satisfies the following residual equation:

$$\mathbf{L}\epsilon^{(1)} = r^{(1)} \quad , \tag{3}$$

where $r^{(1)}$ is the residual associated with $\psi^{(1)}$:

$$r^{(1)} = q - \mathbf{L}\psi^{(1)} \quad . \tag{4}$$

Note that if one has developed a standard Monte Carlo algorithm to solve Eq. (1), the same basic can be used to solve Eq. (2), since only the source function is different. However, one must add the capability to deal with a source that can be both positive and negative. This is relatively straightforward. In particular, one uses the absolute value of the source to generate the probability distribution function. The source particle phase-space coordinates are sampled

using this distribution and the sign of the source is accounted for by having the particle weight carry the sign of the residual source at those coordinates. Once the Monte Carlo estimate for $\epsilon^{(1)}$ is obtained, the solution associated with the first and second batches is formed as follows:

$$\psi^{(2)} = \psi^{(1)} + \epsilon^{(1)} \quad . \tag{5}$$

The process is then repeated for succeeding batches with each batch estimating only the error associated with the solution obtained from the preceding batch. In general, given $\psi^{(n)}$, the solution after batch "n",

$$r^{(n)} = q - \mathbf{L}\psi^{(n)} \quad , \tag{6}$$

$$\mathbf{L}\epsilon^{(n)} = r^{n} \quad , \tag{7}$$

$$\psi^{(n+1)} = \psi^{(n)} + \epsilon^{(n)} \quad . \tag{8}$$

If the error is estimated with sufficient accuracy, each successive batch estimates a smaller component of the solution and exponential convergence is obtained as a function of the number of batches (and hence as a function of the number of particle histories). Because the transport equation is continuous, the angular flux solution has an infinite number of degrees of freedom and hence must be approximately represented in general. For a given angular flux representation, exponential convergence will be obtained until the remaining error in the Monte Carlo solution can no longer be accurately represented, at which point the Monte Carlo solution stagnates at an average fixed error level. We stress that the solution obtained using the ECMC approach *does not represent a standard finite-element solution* but rather represents a least-squares projection of the exact solution onto the trial space. This is in general a far more accurate approximation than a standard finite-element approximation. In standard Monte Carlo calculations, one usually computes projections of the solution rather than the solution itself. For instance, the average scalar flux within a volume represents a projection of the solution. Thus no desired information relating to the solution is nessarily lost by using the ECMC method.

Although we consider source problems here for simplicity, the residual Monte Carlo method can be applied to eigenvalue problems as well. In particular, each power iteration can be performed using the ECMC algorithm. Furthermore, any method developed for one-group problems can be applied to multigroup problems.

3. The Two-Stream Equations

The two-stream transport equations that we consider can be expressed as follows:

$$\frac{\partial \psi^{+}}{\partial x} + \sigma_t \psi^{+} = \frac{\sigma_s}{2}(\psi^{+} + \psi^{-}) + \frac{q}{2} \quad , \tag{9}$$

and

$$-\frac{\partial \psi^{-}}{\partial x} + \sigma_t \psi^{-} = \frac{\sigma_s}{2}(\psi^{+} + \psi^{-}) + \frac{q}{2} \quad . \tag{10}$$

where ψ^{+} $(particles/sec)$ denotes the flux of particles traveling in the $positive - x$ direction, ψ^{-} $(particles/sec)$ denotes the flux of particles traveling in the $negative - x$ direction, σ_t (cm^{-1}) denotes the total cross section, σ_s (cm^{-1}) denotes the scattering cross section, and q $(particles/cm - sec)$ denotes the inhomogeneous source summed over both directions. The

incoming flux value is defined at each spatial boundary. It is not difficult to show that these equations can be algebraically manipulated into the following diffusive form:

$$-\frac{\partial}{\partial x}\frac{1}{\sigma_t}\frac{\partial \phi}{\partial x} + \sigma_a \phi = q \quad , \tag{11}$$

and

$$J = -\frac{1}{\sigma_t}\frac{\partial \phi}{\partial x} \quad , \tag{12}$$

where ϕ is the analog of the scalar flux,

$$\phi = \psi^+ + \psi^- \quad , \tag{13}$$

J is the analog of the net current,

$$J = \psi^+ - \psi^- \quad , \tag{14}$$

and σ_a (cm^{-1}) denotes the absorption cross section. Furthermore, the boundary conditions for the angular fluxes yield Robin conditions for ϕ. This diffusive form makes it fairly easy to obtain analytic solutions for benchmarking purposes. Our two-stream equations are equivalent to the S_2 equations with Lobatto rather than Gauss quadrature. We used Lobatto quadrature to simplify the particle tracking since particles are confined to the x-axis. The ECMC method we outline here can easily be generalized to solve the 1-D slab-geometry S_n equations with quadrature of arbitrary order and type.

4. The ECMC Algorithm

To represent the two stream solution to Eqs. (9) and (10), we begin with a uniform spatial grid having N spatial cells, each of width h, with vertices $x_{1/2}, x_{3/2}, \ldots, x_{N+1/2}$. A standard upwinded piecewise linear-discontinuous representation is assumed within cell i as follows:

$$\begin{aligned} \psi^+(x) &= \psi^+_{i,a} + \psi^+_{i,x}\frac{2}{h}(x - x_i) \quad , \quad \text{for } x \in (x_{i-1/2}, x_{i+1/2}], \text{ all } i, & (15)\\ &= \psi^+_{i-1,a} + \psi^+_{i-1,x} \quad , \quad \text{for } x = x_{i-1/2},\ i = 2, N, & (16) \end{aligned}$$

$$\begin{aligned} \psi^-(x) &= \psi^-_{i,a} + \psi^-_{i,x}\frac{2}{h}(x - x_i) \quad , \quad \text{for } x \in [x_{i-1/2}, x_{i+1/2}), \text{ all } i, & (17)\\ &= \psi^-_{i+1,a} - \psi^-_{i+1,x} \quad , \quad \text{for } x = x_{i+1/2},\ i = 1, N-1 \quad , & (18) \end{aligned}$$

where $x_i = (x_{i-1/2} + x_{i+1/2})/2$, and the vertex flux values are determined for $\psi^+(x_{1/2})$ and $\psi^-(x_{N+1/2})$ by boundary conditions. Note that the trial-space solution that we obtain corresponds to the least-squares fit to the exact solution, $\psi^\pm_e(x)$. This is obtained by evaluating the average and slope in each cell:

$$\psi^\pm_{i,a} = \frac{1}{h}\int_{x_{i-1/2}}^{x_{i+1/2}} \psi^\pm_e(x)\, dx \quad , \tag{19}$$

$$\psi^\pm_{i,x} = \frac{6}{h^2}\int_{x_{i-1/2}}^{x_{i+1/2}} \psi^\pm_e(x)(x - x_i)\, dx \quad , \tag{20}$$

Given average and slope estimates for each cell, the residual is obtained by substituting from Eqs. (15) through (18) into Eq. (4) where **L** in Eq. (4) is defined by Eqs. (9) and (10). One must be careful in evaulating the residual because the discontinuities in the trial-space solution generate delta-function derivatives. For instance, the derivative of ψ^+ is given in cell i by

$$\frac{\partial \psi^+}{\partial x} = \left[\psi^+_{i,a} - \psi^+_{i,x} - \psi^+(x_{i-1/2})\right] \delta^+(x) + \frac{2}{h}\psi^+_{i,x} \quad , \tag{21}$$

where $\delta^+(x)$ denotes a right-sided delta-function :

$$\begin{aligned} \delta^+(x) &= \lim_{\epsilon \to 0} \frac{1}{\epsilon} \quad , x \in [0, \epsilon], & (22) \\ &= 0 \quad , otherwise. & (23) \end{aligned}$$

Assuming a constant distributed source and constant cross sections within each cell, the residual for each direction takes the form of a linear function within each cell together with delta-function sources at each vertex. For instance, in cell i the residual in the positive direction after the n'th batch is given by

$$\begin{aligned} r_i^{+,(n)}(x) = \frac{q_i}{2} + \frac{\sigma_{s,i}}{2}\left[\phi^{(n)}_{i,a} + \phi^{(n)}_{i,x}\frac{2}{h}(x - x_i)\right] - \sigma_{t,i}\left[\psi^{+,(n)}_{i,a} + \psi^{+,(n)}_{i,x}\frac{2}{h}(x - x_i)\right] - \\ \left[\psi^{+,(n)}_{i,a} - \psi^{+,(n)}_{i,x} - \psi^{+,(n)}(x_{i-1/2})\right]\delta^+(x) - \frac{2}{h}\psi^{+,(n)}_{i,x} \quad , \end{aligned} \tag{24}$$

where q_i denotes the distributed source in cell i, $\sigma_{s,i}$ denotes the scattering cross section in cell i, $\sigma_{t,i}$ denotes the total cross section in cell i, and a superscript (n) denotes a quantity evaluated after batch n. It is relatively easy to sample from such source functions, and we have developed a reasonably efficient rejection technique for doing so.

5. Computational Results

We have performed a set of calculations to verify our research code and demonstrate certain fundamental properties of finite-element based ECMC methods. In all calculations the flux moments are estimated using a standard pathlength-based estimator.

Thus, the first problem we consider has the following properties: constant cross-section, with $\sigma_t = 1\ (cm^{-1})$, $\sigma_a = 0\ (cm^{-1})$, $q = 0\ (particles/cm - sec)$, $\psi^+(x_{1/2}) = 0\ (particle/sec)$, $\psi^-(x_{N+1/2}) = 1\ (particle/sec)$, $x_{1/2} = 0\ (cm)$, and $x_{N+1/2} = 1.5\ (cm)$. This problem is intended to verify our algorithm and research code because the exact solution is spatially linear for $\psi^{\pm}$. Thus the solution lies within the trial space, which implies that with any mesh, exponential convergence should be achieved until the ECMC solution is exact to round-off. The error as a function of the number of batches is given in Fig. 1 for 10 cells with 400, 800, and 1600 particles per batch, respectively.

The error is measured in *all* calculations in terms of the scalar flux as follows:

$$error = \sqrt{\frac{\sum_{i=1}^{N}(\phi^e_{i,a} - \phi^{mc}_{i,a})^2 + (\phi^e_{i,x} - \phi^{mc}_{i,x})^2}{\sum_{i=1}^{N}(\phi^e_{i,a})^2 + (\phi^e_{i,x})^2}} \quad . \tag{25}$$

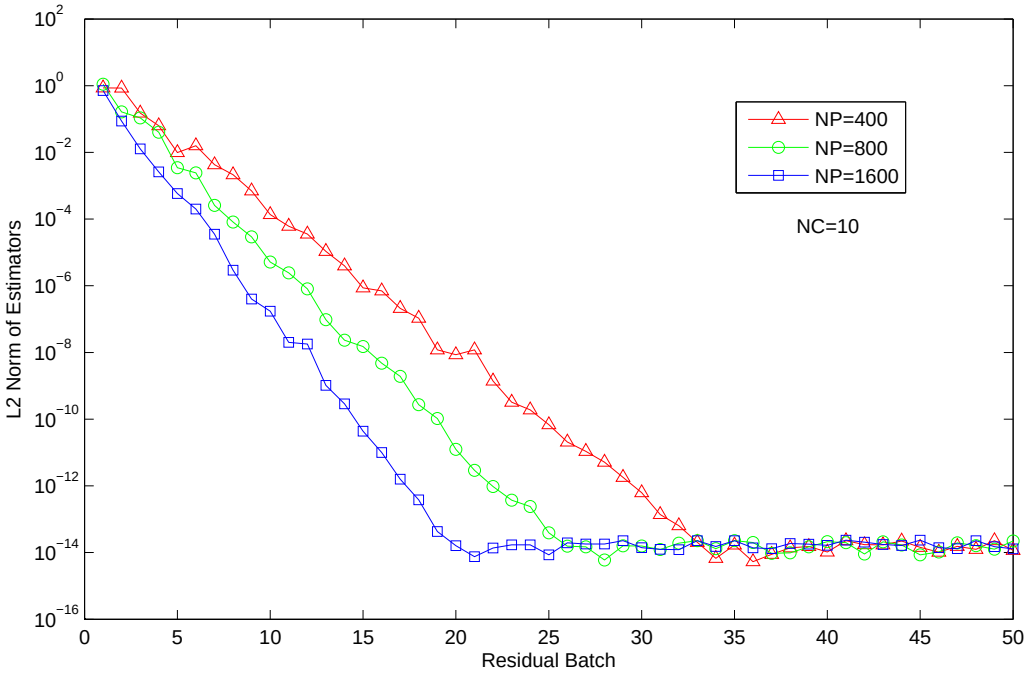

Figure 1: Exponential Convergence for Linear Problem.

where a superscript "e" denotes an exact quantity and a superscript "mc" denotes a Monte Carlo quantity. It is essential to recognize that this measure relates to the error in the average scalar flux and slope within each cell - not the error in the linear-discontinuous representation for the scalar flux within each cell. The scalar flux average and slope can be computed to arbitrary accuracy using standard Monte Carlo given a sufficient number of Monte Carlo histories, but the error in the linear representation will generally not be zero even if the average and slope are exactly known. We choose to measure the error according to Eq. (25) because local integral moments of the solution (such as the cell-averaged scalar flux) are usually of primary interest rather than the trial-space representation for the flux.

There are several important characteristics to be noted from Fig. 1. The first is that the error decreases linearly on a semi-log plot. Thus exponential convergence is achieved. The second is that exponential convergence is achieved until the error reaches the round-off level ($\approx 10^{-14}$) and then saturates. This is expected because the solution lies within the trial space and it strongly indicates that our algorithm and our research code are valid. The third is that the convergence rate increases as the number of histories per batch is increased. This is a very important property. Exponential convergence will only be achieved if a sufficient number of histories are run per batch, i.e., if the error per batch is sufficiently reduced. In our opinion, this makes a very important point about the potential applicablity of the ECMC method. This approach will not make problems that are extremely difficult easier, but it has the potential to reduce the statistical error associated with tenable problems to negligible levels. In addition, this explains why highly oscillatory global polynomial trial spaces can be a very poor choice. The

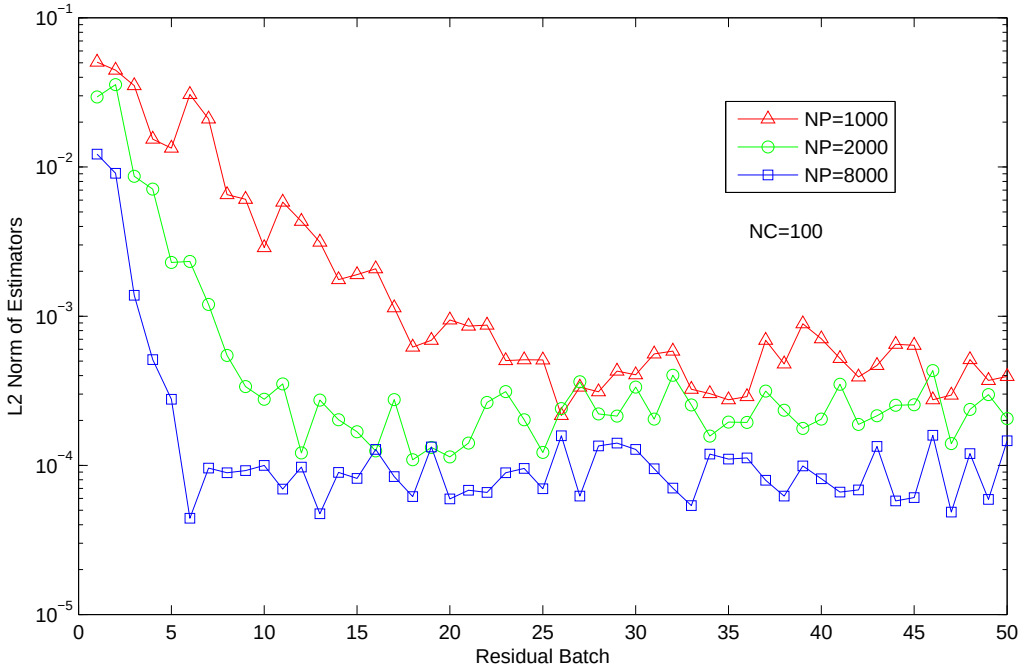

Figure 2: Exponential Convergence with Fixed Number of Particles per Batch.

highly oscillatory nature of the trial space functions yields large and nearly equal positive and negative contributions to the expansion coefficients, resulting in excessive statistical errors that ultimately cause immediate error saturation. Note from Fig. 1 that the error for the NP=1600 case is reduced from roughly one to about 10^{-14} after 20 batches. With standard Monte Carlo, the error reduction after 20 batches would be be expected to be about $1/\sqrt{20} = 4.5$, and 10^{28} batches would be required to achieve the same error reduction as the ECMC method. In this case, the improvement in efficiency with the ECMC algorithm relative to the standard algorithm is astonishing. In general, the efficiency realized for any particular problem will be a trade-off between the extra cost associated with the estimation of the full solution at all points in the problems and the rapid reduction in error achieved with an ECMC algorithm. ECMC algorithms are clearly most promising when the solution is required throughout the problem and the statistical error must be reduced to negligible levels.

The second problem we consider has the following properties: constant cross-section, with $\sigma_t = 1\ (cm^{-1})$, $\sigma_a = 0.5\ (cm^{-1})$, $q = 1\ (particles/cm - sec)$, $\psi^+(x_{1/2}) = 0\ (particle/sec)$, $\psi^-(x_{N+1/2}) = 0\ (particle/sec)$, $x_{1/2} = 0\ (cm)$, and $x_{N+1/2} = 1.5\ (cm)$. The solution to this problem does not lie within the trial space, so the error is expected to saturate at some level as a function of truncation error. The error as a function of the number of batches is given in Fig. 2 for 100 cells with 1000, 2000, and 8000 particle histories per batch. As expected, the error saturates in accordance with the truncation error of the trial space approximation and the saturation error decreases as the number of particle histories per batch is increased. Note that the latter effect occurs because our error measure relates to the error in the scalar flux average and slope in each cell rather than the error in the linear-discontinuous representation for the

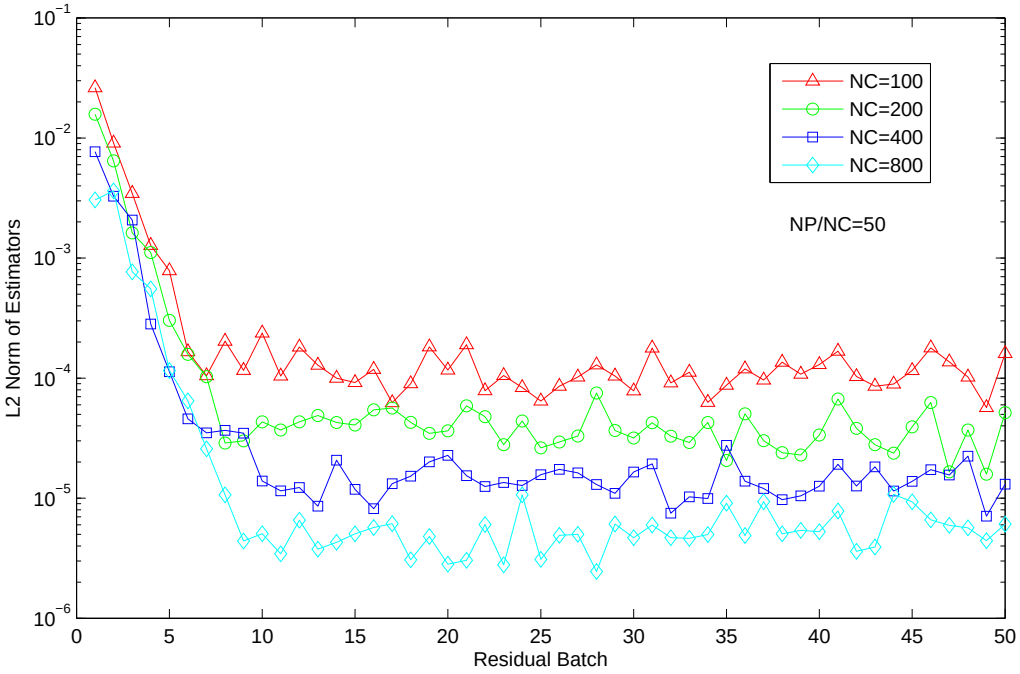

Figure 3: Exponential Converence with Fixed Number of Particles per Cell per Batch.

flux. In the limit as the number of histories per batch increases without bound, the error in the scalar flux averages and slopes will approach zero in the first batch, whereas error in the flux representation will approach a fixed non-zero value.

In our final set of calculations, we again consider the second problem, but we fix the number of particle histories run per batch per cell. The error as a function of the number of batches is given in Fig. 3 for 100, 200, 400, and 800 cells with 5000, 10,000, 20,000, and 40,000 histories, respectively. Since our trial space is second-order accurate, we expected the saturation error to be reduced by a factor of 4 each time the number of cells was doubled. However, the reduction that is seen is less than 4. However, additional calculations (not shown) indicate that as we increase the number of histories run per cell, the reduction in the saturation error approaches 4. Thus this effect is clearly related to combination of statistical error and truncation error.

6. CONCLUSIONS

We have performed a preliminary study of ECMC algorithms based upon finite-element trial spaces. Our initial results are very encouraging and clearly indicate that further research relating to this approach is warranted. The next step should be to develop a theory that quantitatively explains the results that have been obtained for the two-stream equations. Once this has been achieved, a finite-element-based ECMC method for the 1-D one-speed slab-geometry transport equation should be developed. A candidate trial space would have a linear-discontinuous or bilinear-discontinuous dependence on a rectangular space-angle grid. To obtain a highly effi-

cient algorithm, we need to be able to refine the mesh dynamically so that the optimal rate of exponential convergence can be maintained until a desired level of accuracy can be attained. Standard biasing is unlikely to be effective since a globally accurate solution is necessary. A biasing strategy that achieves a relatively constant density of particles throughout the domain would seem to be desirable. We intend to investigate these questions in the near future.

REFERENCES

1. R. Kong and J. Spanier. A New Proof of Geometric Convergence for General Transport Problems based on Sequential Correlated Sampling Methods. *J. Comp. Phys.*, **227**, pp. 9762-9777 (2008).

2. T. M. Evans, T. J. Urbatch, H. Lichtenstein, J. E. Morel . A Residual Monte Carlo Method For Discrete Thermal Radiation Diffusion. *J. Comp. Phys.*, **189**, pp. 539-556 (2003).

3. T. Booth. Exponential Convergence On A Continuous Monte Carlo Transport Problem. *Nucl. Sci. Eng.*, **127**, pp. 338-345 (1997).

4. H. Lichtenstein. Exponential Convergence Rates For Reduced-Source Monte Carlo Transport In [X,Y] Geometry. *Nucl. Sci. Eng.*, **133**, pp. 258-268 (1999).

5. Jeffrey A. Favorite and Henry Lichtenstein. Exponential Monte Carlo Convergence of a Three-Dimensional Discrete Ordinates Solution. *Trans. Am. Nucl. Soc.*, **81**, pp. 147-148 (1999).